Small Angle Gamma Ray Scatter: What Is The Impact On Image Quality

G CUrrie, J Wheat

Citation

G CUrrie, J Wheat. *Small Angle Gamma Ray Scatter: What Is The Impact On Image Quality*. The Internet Journal of Medical Technology. 2007 Volume 4 Number 2.

Abstract

Not unlike the potential small translocation errors associated with the angle of variation from perpendicular defined by the collimator 'hole' length and diameter, limitations of energy discrimination in scintigraphy might also result in a small degradation of resolution and/or contrast.

Methods: A series of 99mTc line sources were acquired with multiple energy windows to provide simultaneous acquisition of data. Each energy window combination was acquired with the line source on the collimator surface, against 4.0cm of water attenuation and against 8.0cm of water attenuation. A series of 99mTc thyroid and brain phantoms were also acquired using dual energy windows positioned to capture a 10% window below 140keV and a 10% window above 140keV. The thyroid and the brain phantoms were each positioned on the collimator surface, against 4.0cm of water attenuation and against 8.0cm of water attenuation.

Results: The mean improvement in FWHM for 140keV + 10% over 140keV – 10% was 0.26mm (95% CI: 0.16 – 0.36) or 4.0% (95% CI: 2.5 – 5.5) which showed a statistically significant variation from the hypothetical zero difference ($P < 0.001$). While a 15% window centred on 144keV provided superior image contrast compared to both 15% and 20% centred on 140keV, the improvement is associated with a decrease in accumulated counts. The increase in sampling error associated with these decreased counts, however, is 0.1% to 0.2%.

Conclusion: Energy discrimination with a symmetric window about the photopeak is ineffective in eliminating photons scattered by as much as 45 to 60 degrees. While the direct impact on image resolution is perhaps negligible, low angle scatter is a major source of potential artifact and contrast degradation. A 15% energy window centered on 144keV might provide an optimized trade-off between contrast and total counts.

INTRODUCTION

The underlying theory for production of a nuclear medicine image appears simple yet the process of image formation is a complex integration of a number of physical principles. Not surprisingly then, any debate on factors influencing image quality in nuclear medicine include reference to photon scatter, attenuation, energy discrimination, spatial resolution, contrast, noise and the like.

SCINTIGRAPHIC ANOMALIES

Gamma camera scintigraphy is confronted by a number of inherent limitations that may impact on the quality or integrity of image data sets. Noise and spatial resolution have already been mentioned. The very nature of nuclear scintigraphy offers another significant limitation. The imaging principle relies on the external detection of radionuclide emissions from deep within a patient. The path of emitted gamma rays can be tortuous or terminal. The interaction of photons in matter are well described in many nuclear medicine physics textbooks; Compton scattering, the photoelectric effect, pair production, photon attenuation and, on occasion, coherent scattering. Imaging relies on physical discrimination (collimator) and energy discrimination (pulse height analyzer) to eliminate object/image photon misalignment. In the case of the former, photons not generally incident perpendicular to the collimator are eliminated. In the case of the latter, photons with significant loss in energy due to scattering which by chance are incident perpendicular to the detector, are excluded from the image.

Despite these measures, a number of anomalies familiar to Nuclear Medicine personnel and attributed to Compton

scattering appear in scintigraphic images. It is a common observation, particularly in the patient with a full figure, on whole body bone scans and whole body gallium scans to note an outline of the body edge that is marginally more intense than adjacent soft tissues. The body halo may also manifest as a line of apparent accumulation in locations of appositional skin (e.g. where the inner thighs meet, the breast fold etc.). The dynamic phase of a bone scan of the hands, when using the cubital fossa as the injection site, often shows what looks like a blood pool image of the hand and forearm prior to actual injection (Fig 1). While anecdotally, these phenomena are attributed to ‘scatter', there is a paucity of discussion in the literature explaining the process whereby scattered photons avoid energy discrimination.

Figure 1

Figure 1: Phantom appearance of radiotracer in the hand and arm prior to actual dose administration.

A PHANTOM

During the course of investigating extraction of 99mTc pertechnetate by grapes, apparatus were conceived to simultaneously measure 99mTc pertechnetate accumulation and water absorption. The grapes were imaged by the vertical gamma camera while suspended above a beaker of 99mTc pertechnetate on a set of scales. The level of 99mTc activity was outside the field of view and shielded using lead. The scales had a purpose build glass housing to minimize the effects of the environment on the accuracy of measurements. For the purposes of these experiments, the lid remained open. Figure 2 shows the scintigraphic image of the apparatus prior to obvious grape accumulation. The glass housing and lid were noted to be prominent despite not containing any radioactive material. The position of the 99mTc below and outside the field of view would require significant scatter of photons to create the appearance; presumably sufficient to result in exclusion by energy discrimination.

Figure 2

Figure 2: Non radioactive glass box with open lid encasing a beaker of 99mTc on a set of scales.

A number of brief experiments were subsequently performed to better define the observed phenomena. A non radioactive glass sheet was positioned perpendicular to the gamma camera. A collimated 99mTc source was positioned in a variety of locations outside the field of view. The gamma camera recorded a vertical distribution of activity corresponding to the glass sheet when the 99mTc source was positioned 10cm or more forward of the level of the collimator (Fig 3).

Figure 6

Figure 4: Brain and thyroid phantoms with target and background ROIs positions used for all 24 phantom studies.

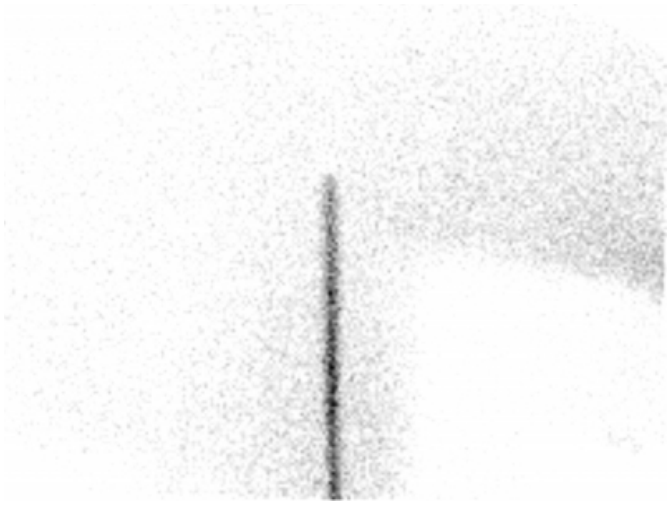

Not unlike the potential small translocation errors associated with the angle of variation from perpendicular defined by the collimator 'hole' length and diameter, limitations of the energy discriminator might also result in a small degradation of resolution. A physical principle rarely discussed with respect to gamma camera energy discrimination is that the residual energy of a scattered photon is a function of the actual starting energy and the angle through which it was scattered. Consequently, higher energy photons will result in a greater percentage loss of energy after scatter through the same angle as a lower energy photon. As an example, a 100keV photon retains 90% of its energy after 60 degrees of scatter while a 5MeV photon will only retain 17% through the same angle (Bushberg 2002). The energy of the scattered photon can be determined by the following equation (Bushberg 2002; Cherry, Sorenson & Phelps 2004):

Figure 4

$$Esc = \frac{Eo}{1 + \frac{Eo}{511}(1 - \cos\theta)}$$

where

Esc is the energy of the scattered photon,

Eo is the energy of the original photon, and

 is the angle through which the photon was scattered.

From this equation it is clear that even 90 degree scatter of a 99mTc photon leaves a scattered photon with an 114keV energy. More importantly in the context of this discussion, a 20% symmetrical energy window about the 140keV photopeak of 99mTc will include photons scattered by as much as 60 degrees (126keV). Reducing the window to 15% will only exclude photons scattered by 45 degrees or greater.

Standard symmetrical energy discrimination about the photopeak is not a useful tool in eliminating small angle scattered photons from subsequent images. Assuming a model where the scattered photon only alters direction once on its path through the body, line of response translocation can range with origin depth from small resolution degrading translocations through to large background contributing translocations.

FURTHER INVESTIGATION

METHODS

In order to determine the impact of scattered photons on image resolution and potential benefits to be gained by alternate energy window strategies, a series of 99mTc line sources were acquired. Line sources were acquired on a Philips Prism 1000 with high resolution parallel hole collimation. A 512 matrix was employed with a 2.0 zoom. Multiple energy windows were employed to provide simultaneous acquisition of data for comparison (table 1). Each energy window combination was acquired with the line source on the collimator surface, against 4.0cm of water attenuation and against 8.0cm of water attenuation. The resulting 198 line spread functions each had the full width half maximum (FWHM) calculated.

Figure 5

Table 1: A summary of energy windows employed in data acquisition.

WINDOW	1	2	3	4	5
20%	126-140 kev	-	140-154 keV	1+3	-
15%	132.5-140 keV	-	140-147.5 keV	1+3	-
15%	132.5-138.5 keV	139.5-143.5 keV	143.5-147.5 keV	1+2+3	2+3

In order to determine the impact of scattered photons on image contrast, a series of 99mTc thyroid and brain phantoms were acquired. Both the planar thyroid and planar brain phantoms were acquired on a Philips Prism 1000 with high resolution parallel hole collimation. A 512 matrix was employed with a 3.2 zoom. Dual energy windows were positioned to capture a 10% window below 140keV and a 10% window above 140keV. The thyroid and the brain

phantoms were each positioned on the collimator surface, against 4.0cm of water attenuation and against 8.0cm of water attenuation. The resulting 18 phantom studies each had regions of interest (ROI) drawn in target and background areas for calculation of image contrast (Fig 4).

Figure 7

Figure 5: Brain phantom with grey matter, white matter and CSF ROIs.

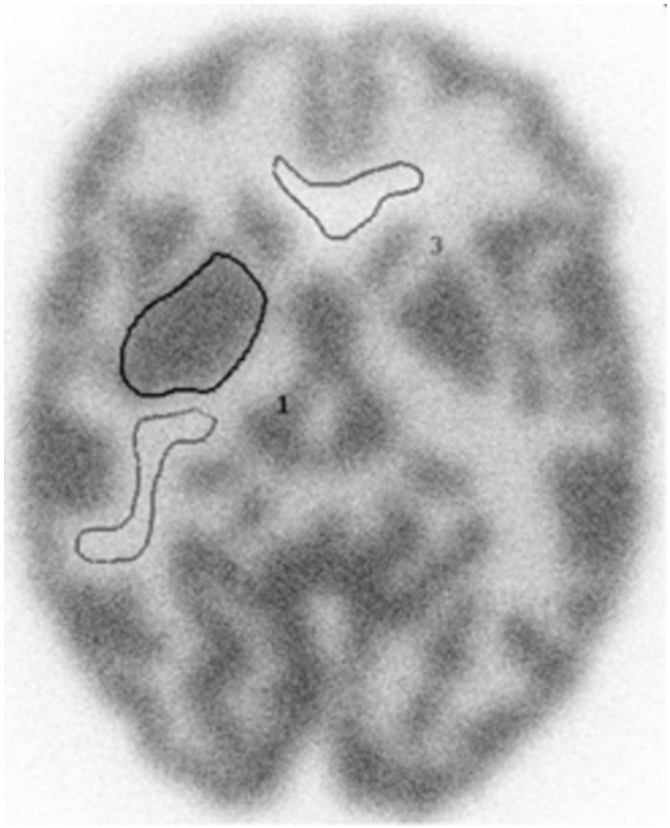

The brain phantom was subsequently imaged to produce three otherwise identical planar studies with a single energy window of; 20% centered on 140keV, 15% centered on 140keV, and 15% centered on 144keV. The resulting images had four ROIs drawn to include grey matter, white matter, cerebral spinal fluid (CSF) and background outside the physical limits of the phantom (Fig 5).

Figure 8

$$C = \frac{(T - B)}{B}$$

The statistical significance was calculated using Student's t test and the F test analysis of variances was used to determine statistically significant differences within grouped data. A P value less than 0.05 was considered significant. The differences between independent means and proportions was calculated with a 95% confidence interval (CI). Image contrast was determined as (Rzeszotarski 1999):

Figure 9

Table 2: Summary of mean FWHM values for each energy window stratified against the attenuation thickness.

WINDOW	1 mean (95% CI)	2 mean (95% CI)	3 mean (95% CI)	4 mean (95% CI)	5 mean (95% CI)
No attenuation	4.35 (4.21-4.49	4.17 (4.01-4.32)	4.21 (4.02-4.40)	4.26 (4.12-4.40)	4.14 (4.02-4.27)
4.0cm attenuation	**6.27 (6.12-6.41)**	6.09 (5.93-6.24)	**5.90 (5.71-6.09)**	6.14 (6.0-6.28)	6.12 (5.99-6.24)
8.0cm attenuation	**8.54 (8.40-8.68)**	**8.18 (8.03-8.34)**	8.27 (8.08-8.46)	8.43 (8.29-8.57)	**8.24 (8.11-8.36)**
P value	< 0.0001	< 0.0001	< 0.0001	< 0.0001	< 0.0001

Where,

C is the object / background contrast

T is the object counts per pixel

B is the background counts per pixel

RESULTS

Not surprisingly, a statistically significant difference was noted between the mean FWHM for no attenuation, 4.0cm of attenuation and 8.0cm of attenuation across all windows (table 2). The P values were supported by a lack of overlap between 95% CIs. While no statistically significant differences were noted in the FWHM between the energy windows for no attenuation (P = 0.368) and 8cm of attenuation (P = 0.0648), window 3 demonstrated a statistically significant improvement in the FWHM over window 1 (P = 0.0175) for the dual window acquisitions. These observations are supported by the overlap (or lack thereof in the case of the latter) in 95% CIs (table 2).

Statistically significant improvements were also noted for window 2 (P = 0.020) and window 5 (P = 0.025) over window 1 at 8cm of attenuation for the triple window acquisitions.

Figure 10

Table 3: Percentage of counts contributed by each energy window.

WINDOW	1	2	3	4	5
20%	55.4%	-	44.6%	100%	-
15%	58.7%	-	41.3%	100%	-
15%	24.1%	49.0%	27.0%	100%	75.9%
20% phantoms	52.6%	-	47.4%	100%	-

The mean improvement in FWHM for window 3 over window 1 using the dual window acquisitions was 0.26mm (95% CI: 0.16 – 0.36) or 4.0% (95% CI: 2.5 – 5.5) which showed a statistically significant variation from the hypothetical zero difference (P < 0.001). No statistically significant variations were noted between the mean FWHM percentage improvements for the different attenuation models (P = 0.254).

The mean improvement in FWHM for window 5 over window 4 using the triple window acquisitions was 0.43mm (95% CI: 0.19 – 0.67) or 6.3% (95% CI: 3.0 – 9.7) which showed a statistically significant variation from the hypothetical zero difference (P < 0.001). No statistically significant variations were noted between the mean FWHM percentage improvements for the different attenuation models (P = 0.422).

Relative count contributions for each energy window indicate that window 1 contributed a greater proportion of counts to the image than window 3 using a dual window acquisition (table 3). Not surprisingly, window 2 using the triple window acquisition had the greatest contribution to total image counts, however, an opportunity to maintain counts and improve image quality might be best exploited by using window 5 or, rather, to use a 15% window centred on 144keV.

Figure 11

Table 4: Percentage of counts contributed by each energy window for the dual window acquisitions for window 1 and 3 and for the triple window for window 5.

WINDOW	1	3	5
No attenuation	51.5%	48.5%	82.4%
4.0cm attenuation	57.8%	42.2%	74.7%
8.0cm attenuation	61.9%	38.1%	70.7%

The impact of distance and attenuation on the inclusion of low angle scatter in an image data set is highlighted in table 4. The relative contribution of window 5 to total counts decreases with increasing distance and attenuation as a result of an increased scatter fraction in window 1. The same observation is made for windows 1 and 3 for the dual window acquisition data.

Figure 12

Table 5: Contrast calculation for each energy window for the thyroid phantom (thyroid versus cold nodule), brain phantom (grey versus white matter) and brain phantom for 8.0cm of attenuation (grey matter versus non phantom background).

WINDOW	1 (126-140 kev)	3 (140-154 keV)	4 (126-154 keV)
Brain (grey v white)			
No attenuation	1.97	2.67	2.27
4.0cm attenuation	1.09	1.90	1.39
8.0cm attenuation	0.79	1.53	1.05
Thyroid (thyroid v nodule)			
No attenuation	6.87	11.8	8.76
4.0cm attenuation	2.47	4.12	3.09
8.0cm attenuation	1.39	2.11	1.69
Brain (grey v background)			
8.0cm attenuation	7.00	37.00	11.00

The brain and thyroid phantoms showed marked improvement in image contrast from energy window 1 to energy window 3 (table 5). Indeed, window 3, with the exclusion of low angle scatter, also provided marked improvements in image contrast over the 20% window centred on 140keV. As a gauge of the actual contribution of low angle scatter to the background noise of an image, the region outside the brain phantom when compared to target counts showed an even more marked disparity between window 1 and window 3 contrast. While a 15% window centred on 144keV provides superior image contrast (table 6) compared to both 15% and 20% centred on 140keV, the improvement is associated with a decrease in accumulated counts within the same time window. The increase in sampling error associated with these decreased counts, however, is 0.1% to 0.2% (table 6).

Figure 13

Table 6: Contrast calculation for the brain phantom comparing 99mTc energy windows for clinical use.

WINDOW	Grey v White	Grey v CSF	Grey v Bkg	Total Counts	Sampling error
20% on 140keV	1.31	3.25	13.78	3388K	1.7%
15% on 140keV	1.48	3.62	16.94	2986K	1.8%
15% on 144keV	1.61	4.22	24.64	2696K	1.9%

Figure 14

Figure 6: Scatter artifact on a SPECT sonogram due to a source external to the patient.

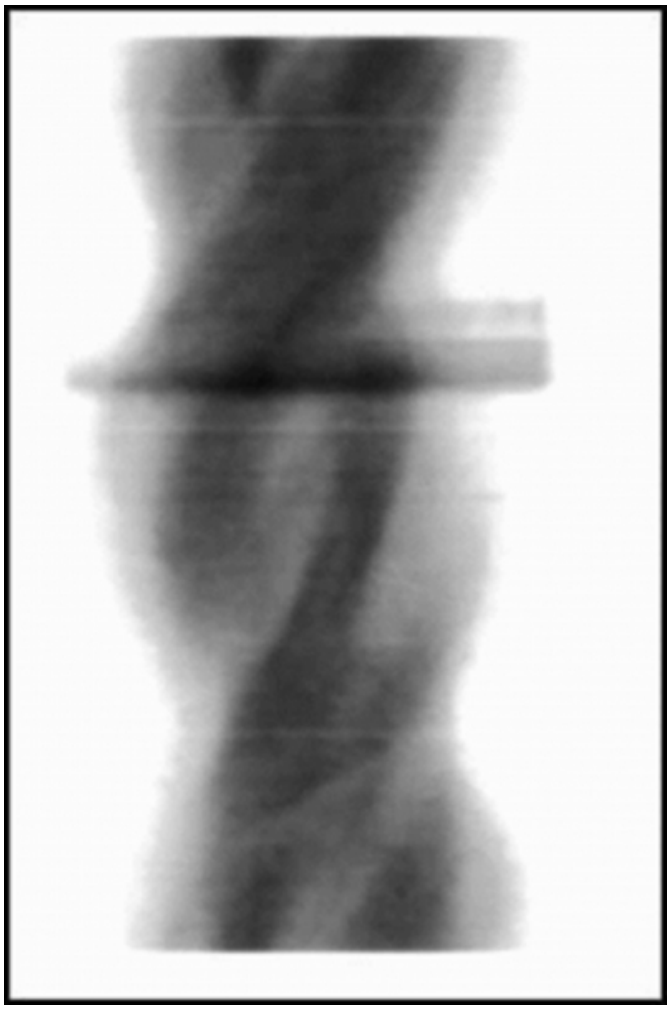

DISCUSSION

Nuclear Medicine professionals make daily protocol decisions that require a trade-off between gains and losses. High resolution versus high sensitivity collimation, two versus three gallium windows, 512 versus 256 matrix, dynamic sampling frames, 8 versus 12 versus 16 gate intervals, and even the choice of a symmetrical 15% window over a 20% window is a trade-off between counts and quality. Perhaps the real benefits from a 15% window are best achieved with an offset above the photopeak (centered on approximately 144keV).

In reality, low angle photon scatter is not likely to cause a discernable difference to image resolution. Comparatively, FWHM in this investigation deteriorated by 2.26mm with the addition of just 4.0 cm of soft tissue attenuation while low angle scatter, even in the worst case scenario, only deteriorated FWHM by 0.36mm. It may, however, present a greater source of artifact than has previously been credited. Artifact may result from other radioactive sources about the patient/gamma camera (eg. patient walking past, dose injection etc.) particularly when multiple gamma cameras share a single room. Figure 6 provides an example of the artifactual appearance of scatter on the sinogram of a gated myocardial perfusion SPECT on a Philips Prism 3000. Furthermore, high background activity and the resulting contrast degradation may result, in part, from low angle scatter through the body. This is consistent with the observed differences in contrast, even for superficial structures, with changes in body habitus. That is, inclusion of low angle scattered photons in the final image is more problematic with greater soft tissue attenuation, an observation familiar to the Nuclear Medicine professional. The high background/soft tissue activity of the obese patient does not simply represent selective retention of the radiopharmaceutical in soft tissue compared to the thin patient. It represents, at least in part, the increased contribution of low angle scatter photons which could be eliminated with a 15% energy window centered on 144keV.

{image:14}

CONCLUSION

When imaging using 99mTc, incident photons contributing to the final image may include photons scattered by as much as 45 to 60 degrees. Energy discrimination with a symmetric window about the photopeak is ineffective in eliminating low angle scatter. While the direct impact on image resolution is perhaps negligible compared to other resolution impediments, low angle scatter is a major source of potential artifact and contrast degradation. The potential impact of low angle scatter on image quality should be given greater consideration in discussion of physical principles in nuclear medicine and in parameter/protocol decision making. A 15% energy window centered on 144keV might provide an optimized trade-off between contrast and total counts.

CORRESPONDENCE TO

Geoff Currie
School of Dentistry and Health Sciences
Locked Bag 588
Charles Sturt University
Wagga Wagga 2678
Australia
Telephone: 61 2 69332822
Facsimile: 61 2 69332866
Email: gcurrie@csu.edu.au

References

r-0. Bushberg, JT, Seibent, JA, Leidholdt, JR and Boone, JM 2002, The essential physics of medical imaging, 2nd edn, Williams and Wilkins, Baltimore.
r-1. Cherry, S, Sorenson, J & Phelps, M 2003, Physics in Nuclear Medicine. 3rd edn, Saunders, Philadelphia.
r-2. Rzeszotarski, M 1999, 'Counting statistics', RadioGraphics, vol. 19, no. 3, pp. 765-782.

Author Information

Geoffrey M. CUrrie, M MedRadSc, M AppMngt, MBA, PhD, CNMT
School of Dentistry and Health Sciences, Charles Sturt University

Janelle M. Wheat, M MedRadSc, D HlthSc
School of Dentistry and Health Sciences, Charles Sturt University